

Magnetic field effects on secondary electron emission during ion implantation in a nitrogen plasma

Ing Hwie Tan,^{a)} Mario Ueda, Renato S. Dallaqua, Rogerio de Moraes Oliveira, and José O. Rossi

Laboratorio Associado de Plasmas, Instituto Nacional de Pesquisas Espaciais, Avenida dos Astronautas 1758, CEP 12227-010 São Jose dos Campos, São Paulo, Brazil

(Received 1 August 2005; accepted 5 April 2006; published online 1 August 2006)

In this work, the magnetic suppression of secondary electrons emitted during nitrogen plasma immersion ion implantation is investigated. Secondary electrons were measured by two Faraday cups with and without the presence of a magnetic field parallel to the target surface. One Faraday cup detects the electrons emerging perpendicularly to the target surface and magnetic field lines, while another cup detects electrons flowing along the field lines. Increase of magnetic field intensity resulted in a decrease of the amount of electrons detected by the perpendicular Faraday cup and in an increase of the electrons detected by the longitudinal one. This shows that secondary electrons were transversally confined by the magnetic field but diffused away from the target ends along the field lines. The secondary electron emission coefficient (γ) was estimated and the results showed that partial suppression (decrease in γ) was achieved when the plasma density was increased by an order of magnitude. We propose an explanation based on the formation of an electron layer (virtual cathode) near the target surface. Better suppression in denser plasmas would be expected because the virtual cathode would be maintained if the electron layer is formed faster than it is longitudinally lost. © 2006 American Institute of Physics. [DOI: 10.1063/1.2201695]

I. INTRODUCTION

Plasma immersion ion implantation (PIII) is a three-dimensional material processing technique¹ that has been developed for various practical applications. The plasma sources used in PIII can either be gaseous plasmas, such as nitrogen used in the nitriding of metals,²⁻⁵ or be generated by vacuum arcs, such as the metallic plasmas used in the implantation of metals in polymers.^{6,7}

Secondary electrons are emitted by target surfaces during PIII due to the bombardment of the energetic ions. At higher ion energies, the secondary electron emission coefficient can be as high as 20, reducing drastically the efficiency of the implantation process. Furthermore, hazardous x rays are produced when the accelerated electrons reach energies above 40 keV and strike the vacuum chamber walls.⁸ Suppression of secondary electrons is therefore an important issue to be investigated in order to improve the efficiency and safety of the PIII process. Electrostatic confinement of secondary electrons has been demonstrated to decrease x-ray emission but without actually suppressing their emission.⁹

Magnetic suppression of secondary electrons in PIII systems was proposed by Rej *et al.*,¹⁰ based on the assumption that a magnetic field parallel to the target surface would confine a layer of secondary electrons near the surface, forming a virtual cathode. Moderate magnetic fields will not alter significantly the incident ion's trajectory nor the work function of the targets, so that suppression would be achieved through the reduction of the local electric field near the target's surface by this virtual cathode, and further secondary electrons emitted in this low electric field environment could

be reabsorbed. Numerical simulations showed that under certain conditions an electron layer would indeed be formed.^{10,11} The crucial point for suppression is that this virtual cathode must be formed faster than it is diffused away along the field lines. If the longitudinal confinement time is not long enough, two beams of transversally confined electrons would be formed along the two directions of the field line.

This concept of magnetic insulation of electrons has been successfully applied to high voltage diodes¹² and intense ion beam accelerators developed for inertial fusion.¹³ Simulations of a magnetic field applied to rf discharges show that plasma density is enhanced by the trapping of secondary electrons around field lines,¹⁴ and the suppression of secondary electrons in divertor plates of magnetic fusion devices has been observed due to the return of electrons within the first gyration around field lines.¹⁵

Since it was published, this magnetic suppression method in PIII systems has not been tested experimentally until recently when we demonstrated in a vacuum arc aluminum plasma that secondary electrons were indeed suppressed by a magnetic field parallel to the target surface.¹⁶ In our equipment, the plasma streams along a straight magnetic duct and a target electrode is positioned with its surface parallel to the duct axis. Two Faraday cups monitoring secondary electrons emitted along and across the field lines did not detect any electrons when the magnetic field was turned on.

Since implantation treatments are often carried out in gaseous plasmas, in this work we extended the experiment to nitrogen plasmas produced in the same equipment but with a dc glow discharge replacing the vacuum arc plasma. Unlike the previous vacuum arc experiment, the plasma in this case

^{a)}Electronic mail: ingtan@plasma.inpe.br

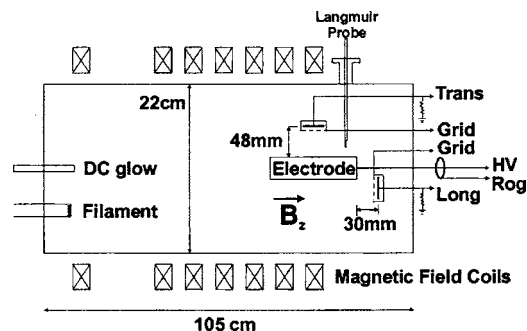


FIG. 1. Schematics of the dc glow discharge system with magnetic field coils, PIII electrode, and Faraday cups (not to scale).

was continuous instead of pulsed, and due to power limitation the magnetic field produced by a dc current supply was limited to 10.7 mT. As in the aluminum plasma case, high voltages were kept below -7 kV due to the pulser's power limitation. Although, at these lower voltages, x rays are not generated, the suppression method's efficiency at higher voltages is discussed. Two Faraday cups were mounted: one to detect secondary electrons that emerge perpendicularly to the target surface while the other monitors electrons that can flow along the field lines, parallel to the target surface. A double electrostatic probe was used to measure the density and temperature profiles of the plasma in both magnetized and unmagnetized discharges.

II. EXPERIMENT

The nitrogen plasma was produced in a 0.22 m diameter and 1.05 m long vacuum chamber, equipped with magnetic field coils around the vessel, as shown in Fig. 1. A dc glow discharge is established between a 7 cm long cylindrical stainless steel rod that is 0.5 cm in diameter and the chamber walls. This rod is typically biased to 450 V, generating plasma currents of $I_p=0.2-0.5$ A (measured by a shunt) at operating pressures around 2×10^{-1} Pa. Under these conditions the plasma potential can reach up to 350 V, which is undesirable in implantation processes due to the sputtering of the target surfaces, which occur between the high voltage pulses. The plasma potential is decreased to less than 100 V by an electron shower from an ac powered tungsten filament immersed in the plasma. The magnetic field coils are powered by a dc current supply, with a field $B=10.7$ mT being produced on the axis when about 25 A of current is supplied to the coils. The magnetic field is uniform in the longitudinal direction to within 5%.

Electron temperature and density profiles were measured by a cylindrical double probe with 6 mm long and 0.5 mm diameter tungsten tips that are 4 mm apart.¹⁷ The voltage between the probe's tips was swept from -90 to $+90$ V, and the I - V characteristic curve (with about 300 points in this voltage range) was monitored. Density and temperature radial profiles were determined at the implantation target's longitudinal position in the presence of the Faraday cups.

A $20 \times 20 \times 50$ mm³ copper electrode was placed in the uniform B region, oriented with its longest dimension along B and the axis of the vacuum vessel. The two 20×20 mm² faces perpendicular to B were hidden from the plasma by

machinable ceramic masks. Three 20×50 mm² faces of the electrode parallel to B were exposed to the plasma. In the remaining parallel face, a machinable ceramic mask exposed a 6×50 mm² strip to the plasma. This copper electrode was biased from -0.5 to -7 kV using a hard tube pulser,¹⁸ with $50 \mu\text{s}$ pulses and 300 Hz repetition rate. The current in this target electrode is monitored by a Rogowski coil with a sensitivity of 0.1 V/A. No arcs or pulsed glow was observed during high voltage pulses.

Two Faraday cups were placed near the copper electrode to detect secondary electrons. The cups are built with a 24 mm diameter circular copper collector and a stainless steel suppressor grid with 30% transparency, 5 mm away from the collector's surface. Both the collector and the suppressor grid are mounted inside a machinable ceramic cup shielded by a grounded aluminum foil. One cup is oriented to collect electrons emerging normally to one of the copper electrode faces (transversal cup). The other cup collects electrons that flow along the field lines (longitudinal cup) parallel to the exposed 6×50 mm² strip. In both cups the suppressor grid was biased to -50 V and a 47 k Ω resistor was connected to the collector in parallel with the oscilloscope input.

III. RESULTS AND DISCUSSION

A series of measurements was made initially with magnetic fields raised up to 4.3 mT and plasma current $I_p=0.3$ A. For higher field values plasma instabilities resulted in large fluctuations in the Faraday cup signals and a significant longitudinal asymmetry decreased the electron density at the target electrode, so that for $B=10.7$ mT no implantation current could be detected by the Rogowski coil. In order to achieve measurable implantation currents at higher magnetic field values, the plasma current had to be adjusted by regulating the filament's current until the I - V characteristic curve of the double probe showed that a maximum electron density was found. For $B=7$ mT, an optimum plasma density was achieved with $I_p=0.5$ A, and for $B=10.7$ mT the plasma current had to be decreased to $I_p=0.23$ A, in order to optimize electron density. The causes for this plasma behavior are under investigation, but despite this variation in plasma conditions, the conclusions with respect to the secondary electrons behavior are still valid.

Figure 2(a) shows the electron density profiles for the first set of measurements with $I_p=0.3$ A in plasmas with $B=0$ and $B=4.3$ mT, with all the apparatus shown in Fig. 1 in place. Note the reduction of the density towards the center where the electrode is located. It can be seen that the density increases with magnetic field as expected. The electron temperature profiles (not shown) are flat increasing with magnetic field from about 4 to 8 eV. Figure 2(b) shows the electron density profiles for magnetic fields $B=0$, $B=7$ mT, and $B=10.7$ mT. From $B=0$ to about $B=7$ mT, with plasma current $I_p=0.5$ A, the density starts to increase significantly at about $B \sim 4$ mT, reaching a maximum at 7 mT, when it is an order of magnitude larger. For higher fields, the density decreases significantly at the longitudinal location of the electrode (not shown), and measurable implantation currents could only be achieved when the plasma current was de-

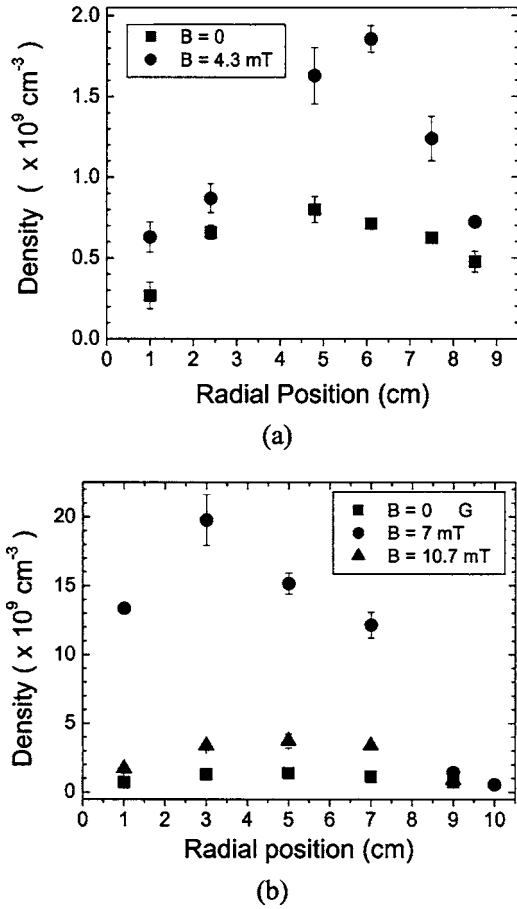


FIG. 2. Density profiles measured with a double probe of plasmas with (a) $I_p=0.3 \text{ A}$, $B=0$ and $B=4.3 \text{ mT}$ and (b) $I_p=0.5 \text{ A}$, $B=0$, $B=7 \text{ mT}$ and $I_p=0.23 \text{ A}$, $B=10.7 \text{ mT}$. Radial distances are measured from the surface of one of the electrode's faces ($r=0$ is radially 1 cm from the vessel axis).

creased (by decreasing the filament current) from 0.5 to about 0.23 A. The electron temperature has a flat radial profile and increases with magnetic field from 3 to about 8 eV. A more complete study of the plasma parameters in the equipment used in this experiment will appear in a future publication.

When a high voltage is applied to the target electrode in the absence of a magnetic field, secondary electrons are emitted

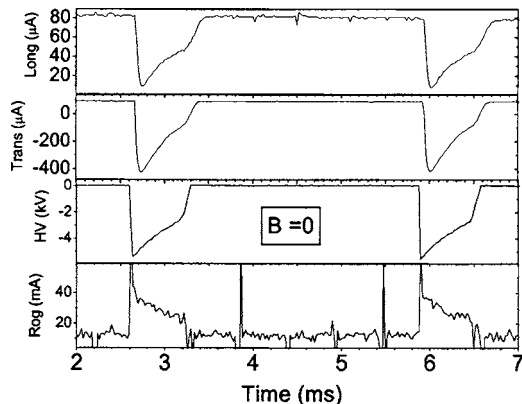


FIG. 3. Temporal evolution of the transversal (Trans) and longitudinal (Long) Faraday cup currents, the high voltage at the target sample (HV), and the current measured by a Rogowski coil (Rog) for unmagnetized plasmas.

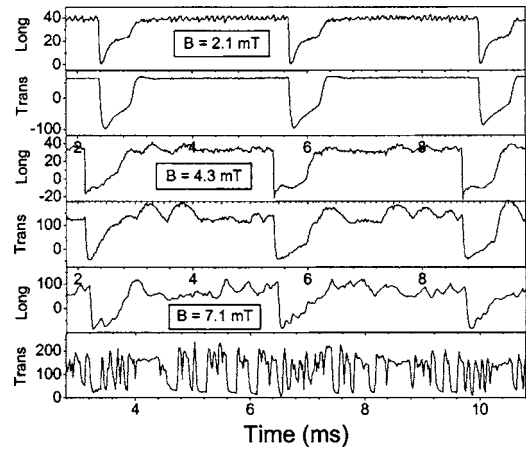


FIG. 4. Temporal evolution of the longitudinal and transversal Faraday cup currents (units in μA) for plasmas with $B=2.1 \text{ mT}$, $B=4.3 \text{ mT}$, and $B=7.1 \text{ mT}$. The high voltage applied to the electrode was about -5 kV in all cases.

ted by the implanted surface and detected by the transversal Faraday cup causing a negative current spike, as can be seen in Fig. 3. Although the high voltage pulse has a $50 \mu\text{s}$ duration, the voltage at the target surface decreases slowly after that, due to the high impedance of the plasma sheath and cabling, until $600 \mu\text{s}$ after the beginning of the pulse, when the pulser circuitry shorts the output high voltage down to zero. Negative current spikes can also be seen in the longitudinal Faraday cup signal, due to secondary electrons emitted at the border of the electrode, where the electric field is not perpendicular to the surface.

When the magnetic field is turned on, the negative spikes in the transversal Faraday cup begin to decrease in amplitude. Near $B=4 \text{ mT}$ the plasma begins to be unstable, and an oscillation starts to grow in the transversal Faraday cup current, as can be seen in Fig. 4. At about $B=7 \text{ mT}$, the negative current spikes are not discernable any more and only the oscillations can be seen in the transversal cup's current. These oscillations are also seen in the longitudinal cup's current with much smaller amplitudes.

Figure 5 shows the amplitudes of the negative current spikes in the transversal cup as the magnetic field is in-

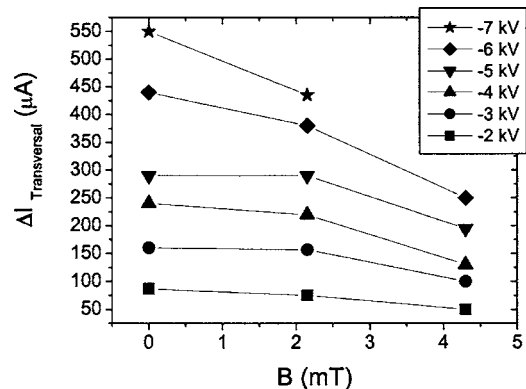


FIG. 5. Amplitude of negative current spikes (from average baseline during high voltage pause to negative peak value during pulses) in the transversal Faraday cup for high voltages from -2 to -7 kV as a function of magnetic field.

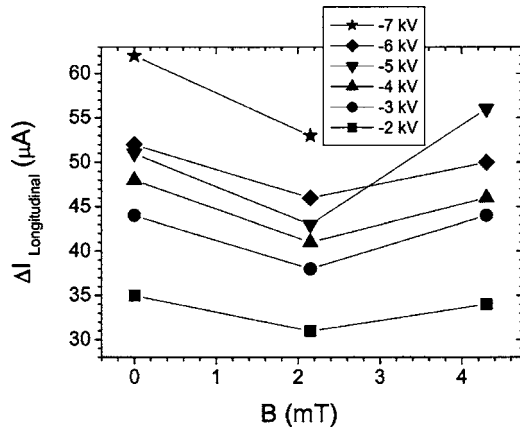


FIG. 6. Amplitude of negative current spikes (from average baseline during high voltage pause to negative peak value during pulses) in the longitudinal Faraday cup as a function of magnetic field for high voltages from -2 to -7 kV.

creased up to 4.3 mT, for high voltage pulses from -2 to -7 kV. There is a clear decreasing tendency of the amplitudes as expected since the electrons are confined by the magnetic field. It should be noted that the amplitudes decrease, despite the fact that plasma density at 4.3 mT is larger than at lower field values.

The behavior of the electrons in the longitudinal direction is more complex than in the perpendicular case. For $B=0$, the negative current spikes measured by the longitudinal cup correspond exclusively to electrons emitted at an angle from the border of the target sample where the electric field during the high voltage pulse is not perpendicular to the surface. When the magnetic field is turned on, the longitudinal cup detects not only the electrons from the border accelerated by the electric field but also electrons from the central region of the electrode that are transversally confined but can diffuse along the field lines. The amplitudes of the negative current spikes measured by the longitudinal Faraday cup are shown in Fig. 6 for the same cases shown in Fig. 5 (high voltages from -2 to -7 kV and magnetic fields up to 4.3 mT). It can be seen that the amplitudes decrease at 2.1 mT, but there is a tendency to increase again at 4.3 mT. This effect could be due to the increase in plasma density with magnetic field, but it could also indicate that secondary electrons that are transversally confined in the central regions of the electrode are diffusing along the field lines and being detected by the longitudinal cup.

To investigate further the increase in the amplitudes of the longitudinal cup's negative current spikes as the magnetic field is increased, another series of measurements was made with magnetic field values up to $B=10.7$ mT, but re-adjusting the plasma current to optimize plasma density in each case. For $B=0$ and $B=7$ mT, the optimum plasma density was found for $I_p=0.5$ A, and for $B=10.7$ mT, the plasma current had to be decreased to 0.23 A (see Fig. 2). Figure 7 shows the amplitudes of the negative current spikes in both the transversal and longitudinal cups as a function of magnetic field, for high voltage pulses of -3.6 kV and -5.5 kV. Despite the presence of large fluctuations in the transversal cup, no negative spikes could be discerned for magnetic

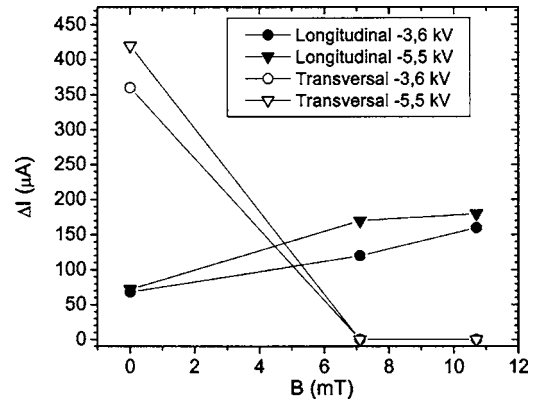


FIG. 7. Amplitude of negative current spikes in the transversal (open symbols) and longitudinal (solid symbols) Faraday cups as a function of magnetic field for high voltages of -3.6 and -5.5 kV.

fields larger than 7 mT. On the other hand, the current due to secondary electrons in the longitudinal cup clearly increases with magnetic field. Assuming that all secondary electrons are transversally confined and form two beams of electrons moving axially away from the two ends of the target electrode, the secondary electron emission coefficient can be estimated and compared with the case without magnetic field.

The secondary electron emission coefficient γ is defined as the number of electrons emitted per incident ion and for singly charged ions it can be calculated as $\gamma=J_e/J_i$, where J_e is determined from the amplitude of the negative current spikes and J_i is determined from the total current measured by the Rogovskii coil $J_{\text{Rog}}=J_i+J_e=J_i(1+\gamma)$. As an example, for the $B=0$ case shown in Fig. 3, the amplitude of the negative current spikes in the transversal Faraday cup is $420 \mu\text{A}$, which divided by the area covered by this cup (4.16 cm^2) and by 0.3 (the transparency of the grid is 30%) gives J_e . The total current measured by the Rogovskii coil is 24 mA, as can also be seen in Fig. 3. Dividing this by the total area of the electrode (33 cm^2) gives J_{Rog} . With the values of J_{Rog} and J_e (known), γ can be calculated giving $\gamma=0.86$ in this case. For $B=0$ and high voltages from -2 to -5 kV, γ was calculated to be from 0.8 to 1.2 (for both voltages), large uncertainties being due to the background oscillations due to plasma instabilities and the low signal to noise ratio of the Rogovskii coil. On the other hand, for $B=7$ mT and $B=10.7$ mT, all secondary electrons are transversally confined and half of them (assuming that two beams are formed flowing away from the electrode in opposite directions along the field line) are detected by the longitudinal Faraday cup as negative current spikes. In these cases J_e is given by the amplitude of the negative current spikes measured by the longitudinal Faraday cup multiplied by 2 and divided by 0.3 (transparency of the grid). As an example, in the $B=7$ mT case shown in Fig. 4, the amplitude of the negative spikes is $170 \mu\text{A}$ while the Rogovskii coil measures a total current of 34 mA giving $\gamma=0.58$.

For $B=10.7$ mT, $\gamma\sim 0.9\text{--}1.2$ for both high voltages (-3.6 and -5.5 kV), similar to the unmagnetized case, which means that in this case there was no secondary electron suppression. For $B=7$ mT, however, the secondary electron emission coefficient is $\gamma\sim 0.3\text{--}0.6$, clearly lower, showing

that in this case secondary electrons were partially suppressed. This is evident since the amplitudes of the negative current spikes is about the same for both magnetic fields (see Fig. 7) but the plasma density is an order of magnitude larger for $B=7$ mT [the total current measured by the Rogowski coil is 34 mA for $B=7$ mT and 24 mA for $B=10.7$ mT, high voltage (HV) = -5.5 kV].

The results obtained so far show that suppression of secondary electrons depends not only on magnetic field intensity but also on plasma density. This is explained reminding that the virtual cathode will be sustained if the rate at which it is formed is faster than the rate at which electrons are axially lost. The surface charge σ in the virtual cathode needed to neutralize the electric field E is $\sigma = \epsilon_0 E$, and the time needed to establish the virtual cathode is $\tau = \sigma / J_e = \epsilon_0 E / \gamma J_i$, where J_i is the incident ion current density and γ is the secondary electron emission coefficient. Since J_i depends on plasma density, the virtual cathode will be formed faster for denser plasmas. This is consistent with the fact that suppression was not achieved at $B=10.7$ mT when plasma density was about $n \sim (2-4) \times 10^9 \text{ cm}^{-3}$ and was partially achieved at $B=7$ mT when $n \sim (1-2) \times 10^{10} \text{ cm}^{-3}$ [see Fig. 2(b)]. Furthermore, the total suppression obtained during the same experiments made in aluminum vacuum arc plasmas,¹⁶ in which plasma densities are even larger ($n \sim 10^{11} \text{ cm}^{-3}$ when the magnetic field is turned on), corroborates this explanation. From the expression $\tau = \sigma / \gamma J_i = \epsilon_0 E / \gamma J_i$, it is seen that at higher voltages (when x rays become important), the electric field will increase proportionally to V and make τ larger, but at the same time the incident ion current J_i (Child-Langmuir space charge limited current) will increase proportionally to $V^{3/2}$, so that suppression should also occur at higher voltages.

The establishment of a virtual cathode will also depend on the rate at which electrons are axially lost. Secondary electrons emerge from the surface with a few eV of energy, in all directions. They are accelerated by the large radial electric field and acquire energies $W_e \sim eE\delta$, where $\delta = 2\nu_E / \Omega$ is the electron layer thickness, $\nu_E = E/B$ is the $E \times B$ drift velocity, and Ω is the electron cyclotron frequency. Minute inhomogeneities and/or scattering can deflect a portion of W_e to the longitudinal direction. It is not clear how plasma density and magnetic field intensity can affect these longitudinal velocities, so more detailed experiments should be made to determine the dependences of magnetic suppression on these parameters.

The values of γ obtained in this experiment can be compared with the available data in the literature. Shamim *et al.*⁸ measured $\gamma=3.9$ for copper targets implanted in nitrogen plasmas with 20 keV ions. We have no knowledge of reports on measurements of the secondary electron yield of nitrogen ions incident on copper targets under the influence of a magnetic field or at lower incident energies, but if γ is assumed to be linearly dependent on ion velocity, it can be approximated by extrapolation according to $\gamma_\phi = \gamma_{20}(\phi/20)^{1/2}$, where ϕ is the ion's energy and ϕ_{20} is the value of γ for 20 keV

ions. This gives $\gamma=1.5-1.8$ for 2–5 keV nitrogen ions,⁸ which is slightly higher than the values obtained.

IV. CONCLUSIONS

For typical plasma parameters of nitrogen PIII systems and moderate magnetic field intensities (up to $B=10.7$ mT in this experiment), the main effect of the application of a magnetic field parallel to the target surface on secondary electrons is to divert their trajectories collimating them into two beams of electrons flowing away from the two ends of the target along the magnetic field lines. Partial suppression was achieved in denser plasmas, probably due to the faster formation of a virtual cathode which reduces the electric field near the surface, inhibiting the emission of more electrons. This explanation is corroborated by the total magnetic suppression of secondary electrons observed previously in an aluminum vacuum arc plasma, in which plasma density in magnetized cases is much larger than in the present case.

The discharge conditions were changed by the magnetic field since electron and ion gyromotions around field lines decrease transport losses, increasing plasma density. On the other hand, with the presence of the magnetic field, a whole class of instabilities can occur so that stable regimes should be searched before considering this method for limiting the emission of secondary electrons. It should also be pointed out that the use of magnetic fields in PIII systems will in general alter the three dimensionality of the process and should be practicable only in two-dimensional applications such as plane or cylindrically shaped substrates.

ACKNOWLEDGMENTS

This work was supported by FAPESP, CNPq, and MCT.

- ¹J. R. Conrad, J. L. Radtke, R. A. Dodd, F. J. Worzala, and N. C. Tran, *J. Appl. Phys.* **62**, 4591 (1987).
- ²M. Ueda, L. A. Berni, R. M. Castro, A. F. Beloto, E. Abramof, J. O. Rossi, J. J. Barroso, and C. M. Lepienski, *Surf. Coat. Technol.* **156**, 71 (2002).
- ³H. Reuther, E. Richter, F. Prokert, M. Ueda, A. F. Beloto, and G. F. Gomes, *Hyperfine Interact.* **156**, 575 (2004).
- ⁴C. Blawert, H. Kalvelage, B. L. Mordike, G. A. Collins, K. T. Short, Y. Jiraskova, and O. Schneeweiss, *Surf. Coat. Technol.* **136**, 181 (2002).
- ⁵J. R. Conrad, *J. Appl. Phys.* **62**, 777 (1987).
- ⁶H. Tan, M. Ueda, R. S. Dallaqua, J. O. Rossi, A. F. Beloto, N. R. Demarquette, and L. Gengembre, *Jpn. J. Appl. Phys., Part 1* **44**, 5211 (2005).
- ⁷Z. Iskanderova, J. Kleiman, Y. Gudimenko, R. C. Tennyson, and W. D. Morison, *Surf. Coat. Technol.* **127**, 18 (2000).
- ⁸M. M. Shamim, J. T. Scheuer, R. P. Fetherston, and J. R. Conrad, *J. Appl. Phys.* **70**, 4756 (1991).
- ⁹D. J. Rej, R. J. Faehl, and J. N. Matossian, *Surf. Coat. Technol.* **96**, 45 (1997).
- ¹⁰D. J. Rej, B. P. Wood, R. J. Faehl, and H. H. Fleishmann, *J. Vac. Sci. Technol. B* **12**, 861 (1994).
- ¹¹K. G. Kostov, J. J. Barroso, and M. Ueda, *Braz. J. Phys.* **34**, 1689 (2004).
- ¹²S. C. Luckhardt and H. H. Fleischmann, *Appl. Phys. Lett.* **30**, 182 (1977).
- ¹³J. P. Van Devender and D. L. Cook, *Science* **232**, 831 (1986).
- ¹⁴S. Rauf, *IEEE Trans. Plasma Sci.* **31**, 471 (2003).
- ¹⁵S. Takamura, S. Mizoshita, and N. Ohno, *Phys. Plasmas* **3**, 4310 (1996).
- ¹⁶I. H. Tan, M. Ueda, R. S. Dallaqua, and J. O. Rossi, *Appl. Phys. Lett.* **86**, 023509 (2005).
- ¹⁷A. Brockhaus, C. Borchardt, and J. Engemann, *Plasma Sources Sci. Technol.* **3**, 539 (1994).
- ¹⁸J. O. Rossi, M. Ueda, and J. J. Barroso, *Braz. J. Phys.* **34**, 1565 (2004).